SHORT RANGE OBSTACLE
DETECTION SYSTEMS

by

Gerald LaBarbera

Rensselaer Polytechnic Institute

Troy, New York

R.P.I. Progress Report MP-6

SHORT RANGE OBSTACLE DETECTION SYSTEMS

by

Gerald LaBarbera

NASA Grant NGL 33-018-091

Analysis and Design of a Capsule Landing System and Surface Vehicle Control System for Mars Exploration

September 1969

Rensselaer Polytechnic Institute
Troy, New York

ABSTRACT

This report represents a feasibility study of an electro-optical obstacle avoidance system for use on a possible future N.A.S.A. Martian roving vehicle. The proposed system makes use of the range finding abilities of a single lens and the focus detecting properties of the Cadmium Sulphide (CdS) photocell. By application of the equations of geometric optics, the lens characteristics are related, mathematically, to certain properties of the detector. Next the theory of operation of the CdS cell is investigated in the context of its ability to detect focus. Several experiments were performed to ascertain its ability to carry out the necessary functions of an onboard focus detector.

The results indicate that: (1) the optical approach to range finding is basically sound if a suitable focus detector can be found; (2) The CdS cell falls far short of being the sort of detector needed in such a system for operation on Martian terrain.

The failure of CdS cells as a focus detector should not detract from the optical focusing method. This system remains the only one of several considered that becomes more accurate as the range shortens. Possibly the solid state vidicon (Ref. 1) could be the focus detector that makes the system practical.

TABLE OF CONTENTS

LIST OF FIGURES

I. INTRODUCTION

For an unmanned roving vehicle on the surface of Mars, the distance of the vehicle from Earth will be approximately 150,000,000 miles which essentially precludes its being directed by controllers on Earth due to the 10 minute transit time for radio signals.

This situation makes it mandatory that the vehicle contain an onboard decision making system that will handle many of the point-to-point navigational functions of the vehicle. One of the most important problems facing this system will be that of obstacle avoidance.

The photographs taken on the Mariner fly-by missions have revealed a surface which has many similarities to that of the moon except for atmospheric weathering. The hazards presented by the Martian surface are complicated by the presence of sand storms and generally unstable atmospherics.

The surface features can be lumped into two broad classifications, namely, positive and negative, which are defined as follows. Details which can be perceived directly by a line-of-sight detector are said to be positive while those which make their presence felt by lack of direct perception are considered negative. Figure 1 indicates positive and negative terrain features as seen by a line-of-sight detector. An obstacle is considered to be a feature which the vehicle cannot negotiate directly and must initiate maneuvers to avoid.

To date, most avoidance systems considered have used positive feature obstacle detectors (line-of-sight detectors); negative features being assumed wherever positive features are absent until a new vehicle position provides new data to fill in the gap. These systems fall into three categories: (1) mechanical, (2) acoustic, and (3) electromagnetic.

The use of mechanical "feelers" is almost mandatory for this type of vehicle. This is the only system capable of detecting both categories of features and would most likely operate within a distance of about six feet in front and to the sides of the vehicle. Its basic shortcoming lies in the fact that the vehicle must approach to within a few feet of a feature to decide if passage is possible. This would most likely entail many reversals of direction with the attendant physical dangers and wear associated with this maneuver. This situation creates a necessity for a longer range method of obstacle sensing (possibly thirty feet) to augment a mechanical system.

An acoustic system, similar to sonar, was contemplated by Wright (Ref. 1). However, this approach was rejected because the high wind velocity, when coupled with the low Martian atmospheric pressure, approaches the velocity of sound.

A radar system is one possible form of electromagnetic obstacle detection. The relatively short distances involved, however, cause timing difficulties due to inherent delay and

saturation times (Ref. 2).

Another possibility is a laser range finder. In this case, pulses of coherent light are transmitted and their timed return gives the range of the object. This method seems to hold more promise than the radar system and as such, is the subject of a parallel effort at Cornell University.

Alternatively, an approach using passive optical ranging was proposed by Wright (Ref. 1) and will be pursued further in this report. The configuration to be studied is a single lens system with a focus detector. Briefly, the method to be studied is based upon the fact that when a lens is focused on an object a simple relationship exists between the image distance, focal length, and object distance. The knowledge of any two of these quantities allows the computation of the third (Figure 2a). For a particular lens, the focal length is fixed and if the image distance can be determined by bringing the lens into focus, the object distance can be calculated.

The first part of this report relates the optical parameters to the problem of range finding by focus detecting. Sample calculations are presented to give the reader a feel for the magnitudes involved. While no focus detector is specified, the general qualities of an acceptable detector are established.

The second part deals with the investigation of Cadmium Sulfide (CdS) photocells as a detector. The effects of the cell's geometry are discussed and several experiments are described which illustrate the strong and weak points of the CdS photocell as a focus detector.

II. THE OPTICAL SYSTEM

Optical Relationships

A simple lens will focus the light rays from a point on an object in one plane (object plane) into a point in an image in another plane (image plane) as shown in Fig. 2a. The distances of the object and image planes from the lens are related to the focal length of the lens by the following well-known equation:

$$\frac{1}{U} + \frac{1}{V} = \frac{1}{F} \qquad (1)$$

where F is the lens focal length, U is the distance of object plane from the lens, and V is the distance of image plane from the lens.

This relationship holds for all objects outside of the lens focal length and gives a method of determining the object's distance from the lens as long as the focusing of the lens can be detected. Ideally, the image plane (plane of best focus) is unique and readily determined if the values of F and V are known. The situation is complicated, however, by the

existence of the depth-of-field effect. This effect causes the image to appear in focus over a range either side of the plane of best focus (Fig. 2b). In normal photographic work, this effect is highly desirable but it is a definite disadvantage in the application being considered here.

When considering the depth-of-field effect on the image side of the lens it is useful to define the circle-of-confusion as the circle formed by a point image on any plane other than the plane of best focus. The diameter of the circle-of-confusion increases as the plane under consideration is moved further from the plane of best focus (Fig. 2b).

When referring to the object plane, the depth-of-field is the distance through which the object can be moved without significant defocusing of the image in the plane of best focus. Obviously, some definition of what is meant by "significant" defocusing must be given if these effects are to be discussed quantitatively. Usual photographic practices (Ref.3) indicate that a circle-of-confusion having a diameter of .01 inch will result in perfect focus insofar as the human eye can detect. This figure will be used later in a sample lens calculation. For maximum resolution in this type of obstacle detector, it is desired that the depth-of-field be as shallow as possible. For a given lens, the depth-of-field is shallowest near the lens and gets progressively deeper as the object distance increases.

The manner in which the focusing properties of a lens

can be applied to the problem of obstacle detection is demonstrated in Fig. 3. Four photographs were taken of a terrain model with a camera having an F 1.4 lens of 40 mm focal length. The location of the object plane is determined by the focus setting on the camera. As the object plane is passed through the three-dimensional scene from front to back, details pass in and out of focus. In principle, if those objects which are in focus can be detected, their ranges from the vehicle can be computed. However, as the focus setting increases, the depth-of-field does also, to the extent that the position of the object plane has become somewhat ambiguous in the last photograph. The final photograph covers as much depth as the previous three photos combined.

System Design Considerations

In order for any range finding system based upon focus detection to be practical, it must maintain a shallow depth-of-field at distances to twenty feet or so while still covering a minimum azimuth angle of perhaps 60°. If the lens is to handle an angle of this width without mechanical scanning, the focus detector may have to be very acute, in the sense described below.

Acutance in the focus detector is now defined as the minimum diameter of the circle-of-confusion that the detector can distinguish from a point image. Implicit in this definition is the assumption that the ability of a device to

detect the focusing of an image is expressible in terms of its ability to detect the focusing of a point source. Because the depth-of-field is greater on the far side of the object plane, the distance U_2 in Fig. 14 will be used in the calculations because it represents the worst case for focus detection.

The angle-of-view and the focal length are related by (Ref. 3).

$$\alpha = 2 \text{ arc tan } \frac{b}{2F} \tag{2}$$

where α is the angle-of-view when the lens is focused at infinity and b is the size of the image. For an angle-of-view of 60^{o} and an assumed image size of 5 in. x 5 in., it follows from (2) that the focal length must be 4.33 in.

Having determined a value for the focal length of the lens, then the relationship between the lens diameter and the diameter of the circle-of-confusion may be found by considering the required depth-of-field. It is shown in Appendix I that these parameters are related by the following expression:

$$D = d \frac{U_2 \ (U - F)}{F \ (U_2 - U)} \tag{3}$$

where D is the lens diameter and d is the diameter of the circle-of-confusion. If it is desired to have a far depth-of-field of 2 ft. at a range of 20 ft. with a focal length of 4.33 in., it follows from (3) that

$$D = 609 \ d \tag{4}$$

Hence, the larger the circle-of-confusion required by the focus detector, the larger the lens must be in order to satisfy the depth-of-field requirement. If it is assumed that the detector will function for d = .01 inch (slightly better than the human eye), the resulting lens diameter would be 6.09 inches. This size may or may not be practical depending on the structure of the vehicle. If the only focus detectors available require a circle-of-confusion with diameter greater than .01 inch, it would seem prudent to consider alternate approaches, such as scanning the image. If the lens diameter must be reduced, the angle-of-view must be reduced, all other factors remaining fixed.

It has been suggested that if the optical system must be aimed in some manner, it would be prudent to restrict the angle-of-view such that only one detector would be required for focus detection. Clearly, it would be cumbersome to physically aim the entire system. However, the same effect is attainable by other means.

For example, a mirror mounted on gimbals in front of a stationary optical system can produce a scan of a wide area while affording a minimal moving mass. One possible arrangement would involve a vertically mounted optical system topped with a periscope type of structure. An inherent advantage of this configuration is the possibility of system operation in the event the vehicle must reverse its direction of travel.

There are three primary methods of focusing the system. They are: (i) moving the lens; (ii) moving the detector; and (iii) changing the length of the light path by moving an intermediate mirror or prism.

The first approach has the advantage of being accomplished by rotary motion alone. This allows for a rigid structure that is very vibration resistant. Its principle disadvantage is that it involves the motion of the relatively massive lens system.

The second method has the advantage of being light in weight and still affording reasonable structural rigidity. However, the motion would involve the stressing of delicate electrical connections which would present an important reliability consideration.

The third approach is free of electrical connections and is relatively light in weight, but is complicated in nature and apt to be fragile. A choice among the three approaches could only be made with a knowledge of the vehicle space problems, lens size required, and type of detector used.

From the foregoing, it would seem safe to assume that a focusing range finder is physically realizable if a suitable focus detector can be found. The second portion of this report deals with one such detector.

III. THE DETECTOR

Material Properties

Cadmium sulphide (CdS) photocells have an interesting

non-linearity associated with their operation. The resistance of these photo-conductors not only varies inversely with the magnitude of the illumination on their surfaces, but also varies in like manner with the amount of area covered by the illumination. This effect can be seen in pictorial form in Fig. 4. Here a point source of light is defocused so as to cover succeedingly larger areas of the cell's surface. The accompanying graph indicates the change in cell resistance as this defocusing takes place. It is this effect that was investigated as a possible focus detecting property. Inasmuch as any image can be considered an infinite number of discrete points, it was felt that the CdS cell's reaction to point sources might be carried over to a more complex image and allow the device to serve as a focus detector. Realizing that super-position does not apply to a non-linear device and that other attempts (Ref. 7) at focus detecting using CdS cells have met with only limited, special-case success, a test program was initiated with simple point images and progressed to complex terrain images in steps small enough to get an emperical profile of the cell's performance.

It might be mentioned here that one company (Ref. 7) is now producing a device that utilizes the CdS cell as a focus detector on a simple line image. In this case the cell is equivalent to the human eye aided by about thirty diameters of magnification.

Mathematical Model

Several investigators (Refs. 4,5,6) have addressed themselves to the problem of explaining the focus detecting abilities of the CdS photocell. The following is a simplified, linear model that explains how focus detecting can occur with a line target.

The local conductance in each part of the photoconductive layer is directly proportional to the local illumination. The photoconductive surface of the cell is thought of as forming a conductor matrix, such as is represented in Fig. 5. Elements in the matrix are considered to be particles (perhaps grains) in the sintered photoconductor, each of which reacts independently to the light incident upon it.

Assume the matrix to have m columns and n rows. For simplicity, each elemental conductor in the matrix is assumed to be very much smaller than the smallest relevant details in the image of the target. Assume that each line of the target covers an integral number of conductors in the matrix and that the conductors (g_{aa}, g_{ab}, ... etc.) which are parallel to the terminals have little effect on the conductance between terminals.

The terminal conductance of the matrix is now considered for three different cases:

(i) A uniform filter in place of the target;

(ii) The filter is replaced by a Ronchi ruling (see Fig.6) having the same total transmittance as the filter

used in (i). The lines of the projected image are perpendicular to the terminal electrodes (see Fig. 7);

(iii) Same as case (ii) but the lines of the projected image are parallel to the terminal electrodes (see Fig. 8).

The conductances for the three cases are derived in Appendix III and are given by

$$G_1 = g_o \left(\frac{m}{n}\right) L \tag{6}$$

$$G_2 = \frac{1}{2} g_o \left(\frac{m}{n}\right) (L_D + L_L) \tag{7}$$

$$G_3 = 2 g_o \left(\frac{m}{n}\right) (L_D L_L / (L_D + L_L)) \tag{8}$$

here g_o is the conductivity of each elemental conductor in darkness, m and n denote the size of the matrix, L_D is the illuminance of the dark line, L_L is the illuminance of the light line and $L = L_D + L_L$.

Since $L = L_D + L_L$ it follows that $G_1 = G_2$ and no differences should be noted between case (i), even illumination, and case (ii), where the in-focus line image is oriented perpendicular to the terminal electrodes. On the other hand, case (iii), where the in-focus line image is parallel to the terminal electrodes, will cause a substantial difference to occur in the terminal conductance. Hence, any process that begins with case (i) and ends with case (iii) i.e., the focusing of a line image, should cause a noticeable change in cell conductance

and hence one should be able to detect the focus condition from measurements of the conductance.

Actual experimental results with line targets differ from those stated above because of secondary non-linearities present in an actual cell. These results will be treated in a later section.

Cell Structure and Preparation

One of the first steps to practical experimentation was to acquire a simple area cell of the type shown in Fig. 11. This proved to be a different task, since most manufacturers produce cells with a serpentine type of sensitive area, similar to those in Fig. 9. The purpose of this geometry is to circumvent the very effect we were investigating. It allows the CdS area to be optically shorted quite easily so that the cell as a whole acts as if it were sensitive to the magnitude of illumination only and not to the distribution of the light.

After much searching, two types of simple area cells were found. One cell was about 1/4 of an inch square and came with an integral plastic covering. This covering caused much internal reflection which made the cell useless for our purposes. The other cell was about one inch in diameter and was actually the same chip as found in the largest cell in Fig. 9, but it had been removed from production before completion of the manufacturing process. It was this cell which was modified and used in the following experiments.

An optical bench was set up, holding a light-tight enclosure within which the test cells were mounted. The cells could be tested with line targets, light sources, and terrain models constructed on a modeling table. Figure 10 shows the set-up using the National Bureau of Standards resolution chart as a target.

The cell itself was processed in the following manner. First, gold contacts were evaporated on the edges to a depth of 700 Angstroms. Second, copper wires were attached to the gold with indium solder. Last, the ceramic chip was cemented to an aluminim disc suitable for mounting in the three point lensmounts used on the optical bench. The finished product appears in Fig. 11.

Experiments

All of the following experiments were done using the optical bench and an F3.5- 75mm lens. In all cases the lens was moved to obtain focusing, thereby keeping the object-to-cell distance constant. Resistance measurements were made by using an analog ohmmeter and, where accuracy was needed, a digital ohmmeter with better than 1% accuracy.

The serpentine cell, when presented with an image made up of alternating 1/16 inch light and dark lines (Fig. 12), resulted in the resistance changes as shown in Fig. 12b. If the image is parallel to the CdS stripe, the solid line is the result; if perpendicular, the dotted line is the result.

These, along with light source imaging, were the only results ever noted from the serpentine structure.

Figure 13 is a plot of the resistance change when the same line image was presented to the area cell. Here the solid line resulted from the parallel orientation and the dotted line, the perpendicular orientation, each with respect to the terminal conductors.

The results closely resemble the original matrix model. The peak is sharp and well defined and all indications are that the CdS cell would make a fine focus detector for this type of target. Results are similar for other line and dot targets that approach a 50-50 light and dark distribution with high contrast. In every case, the cell orientation has proven important and affects the peak amplitude, but has little effect on the peak location relative to the plane of best focus.

Tests made using amorphous and complex random targets such as craters constructed on the terrain modeling table were, on the other hand, completely unsuccessful. Results on such images were completely negative in the sense that no measurable changes of resistance were detected as the lens was moved. There seems to be very little middle ground between the two extremes; either it works well or not at all.

CONCLUSION

Optical System

The optical system for range finding by focus detecting

seems physically realizable if a suitably acute focus detector can be found. The exact form of the optical system would be determined by the vehicle and detector parameters.

Detector

From the foregoing data, one must conclude that the CdS photocell would not perform well as a focus detector in the topological environment of Mars. Here it must be stated that one important variable not under direct control in this experiment was cell structure. While geometry could be varied, there was no way to vary the material constituency of the cells or the processes by which they were made. It was felt, however, that the CdS material used in these cells was very representative of modern, panchromatic sulphides.

Future Work

The failure of the CdS cells as a focus detector should not detract from further study of the optical focusing method. This system remains the only one of several considered that becomes more accurate as the range is reduced. Possibly the solid-state vidicon mentioned in Ref. 1 could be the focus detector that makes the system practical.

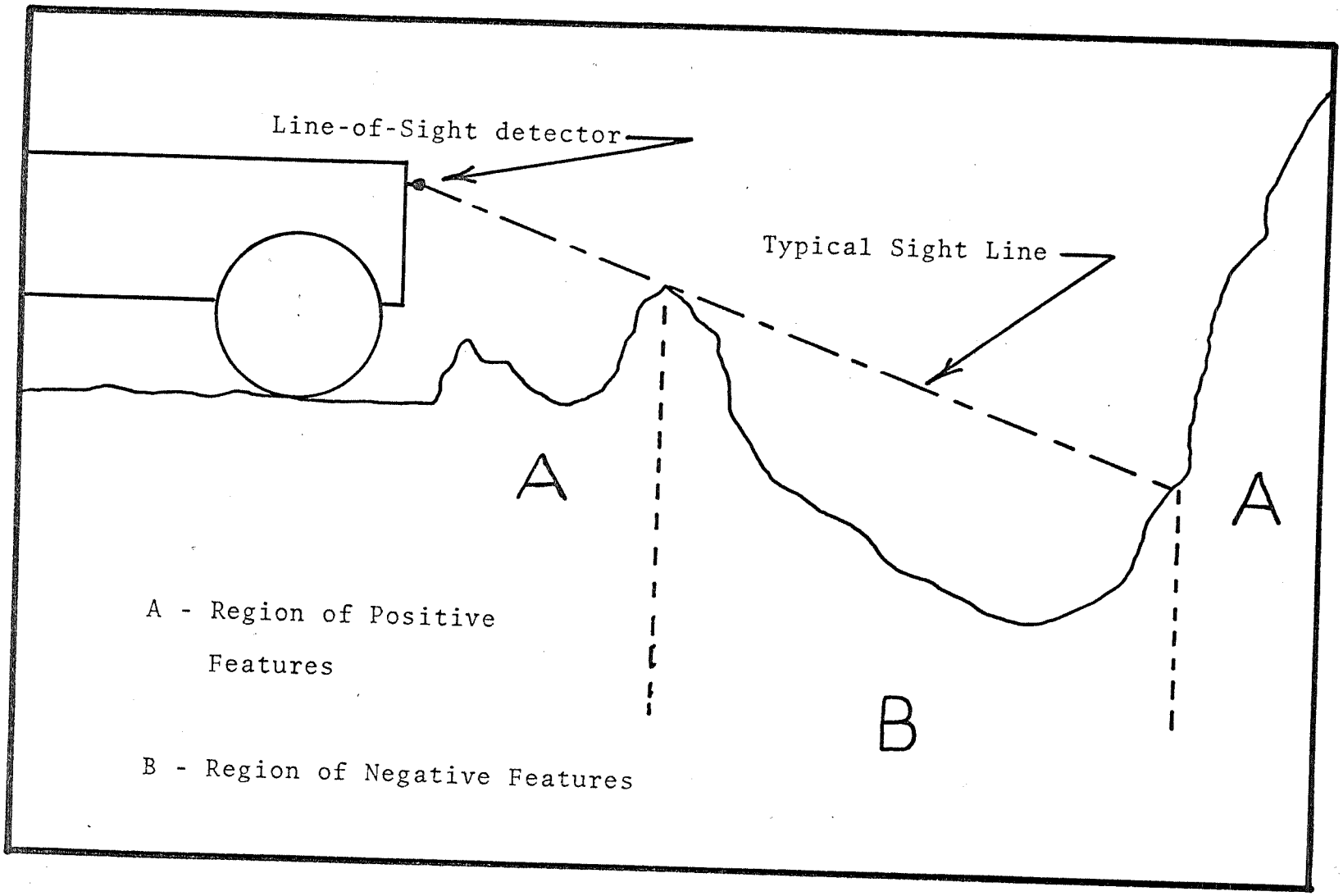

FIGURE 1 - Positive and Negative Terrain Features

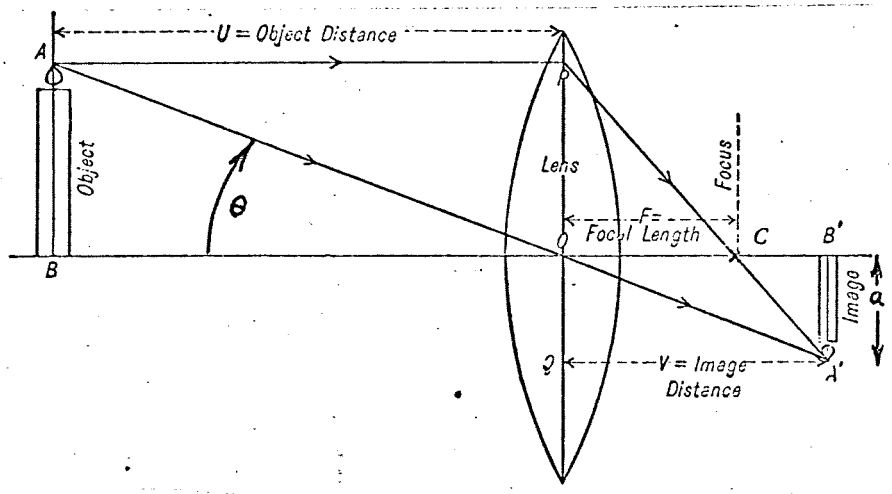

(a) Optical Parameters

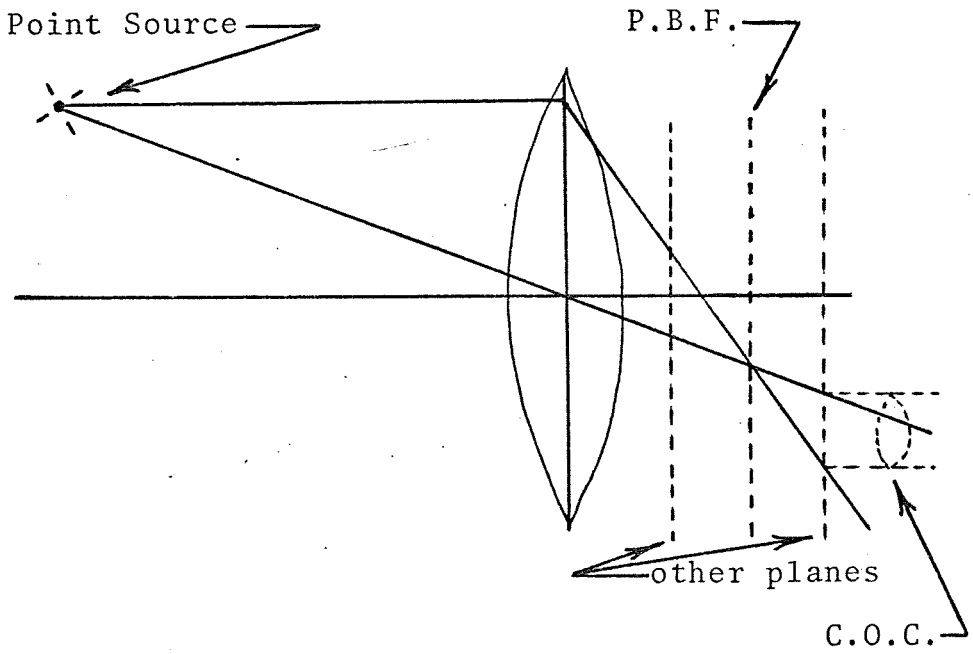

(b) Circle of Confusion (C.O.C.)

FIGURE 2 - Simple Lens Relations

(a) 0.45 meter

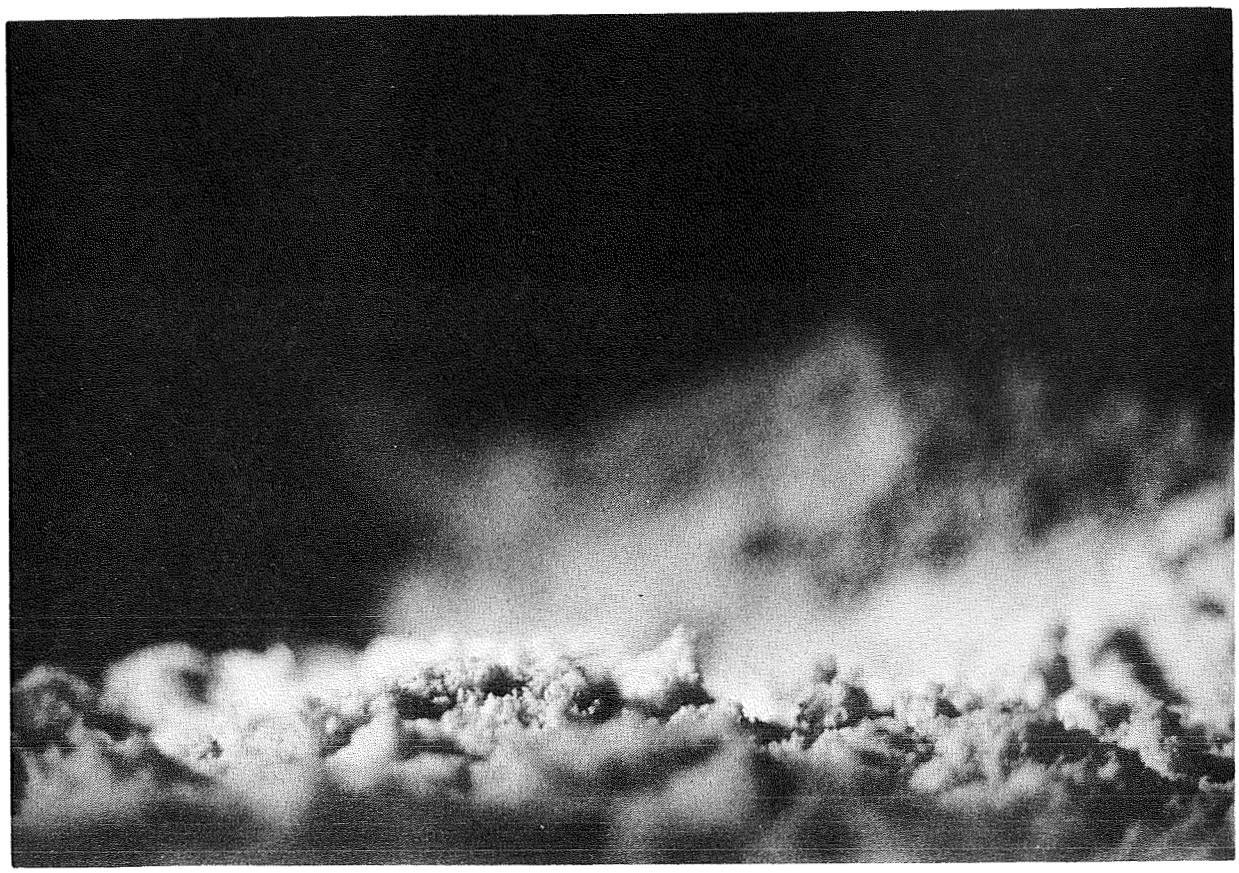

(b) 0.55 meter

Figure #3 Depth-of-Field Effects in a Terrain Model

(c) 1.10 meter

(d) 0.85 meter

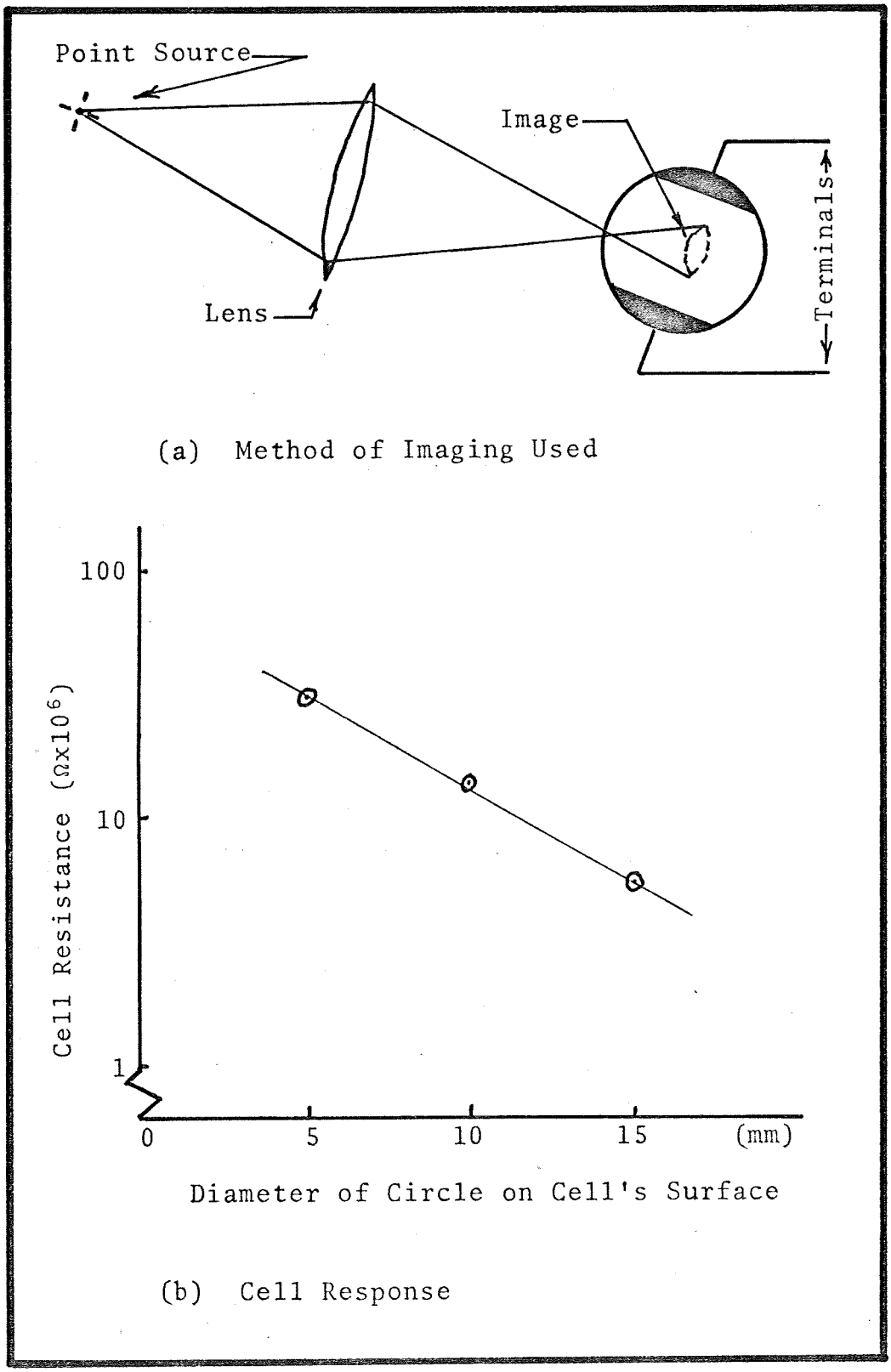

FIGURE 4 - Response of "Area" Cell to a Point Source

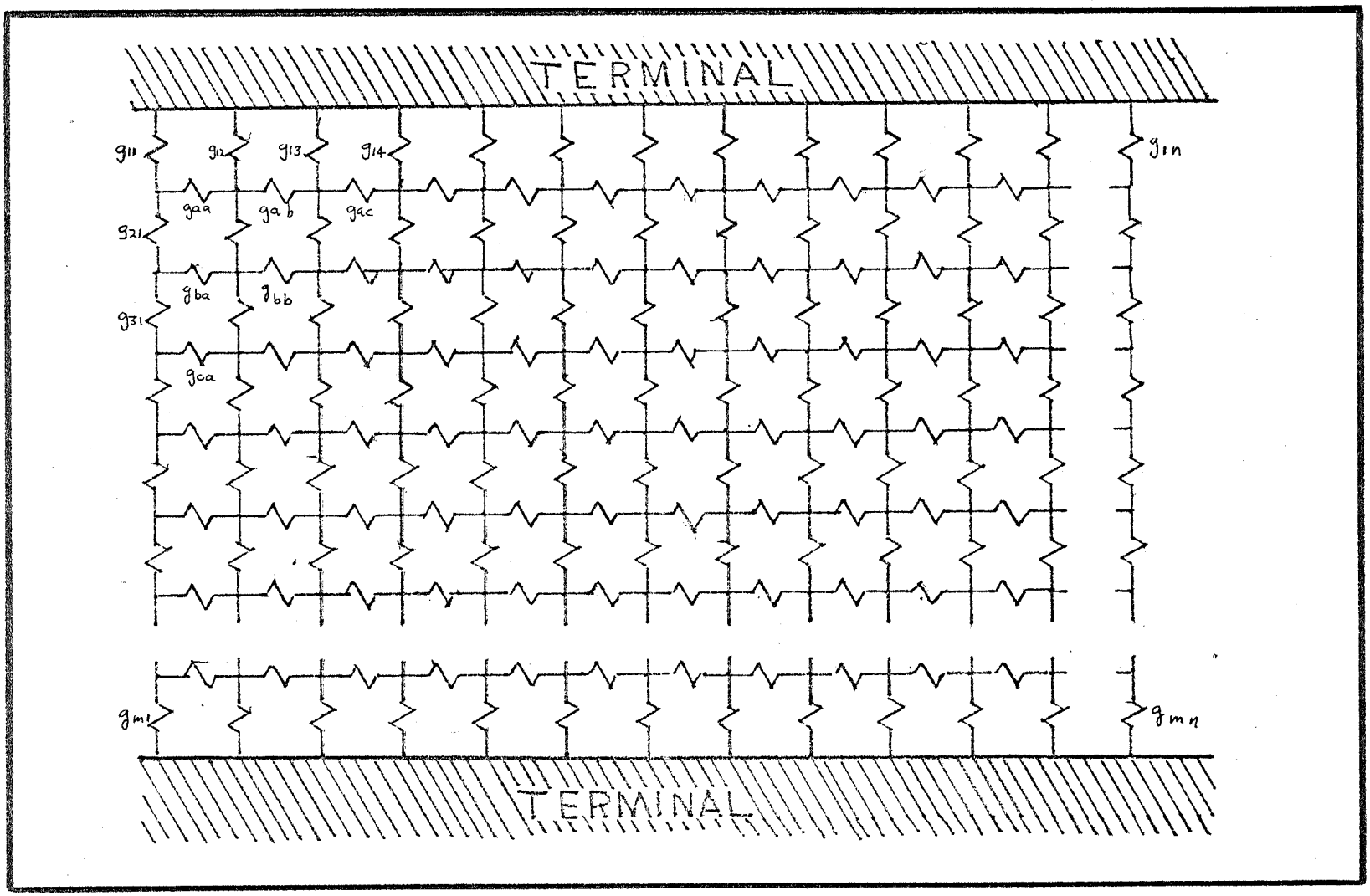

FIGURE 5 - Mathematical Model Matrix

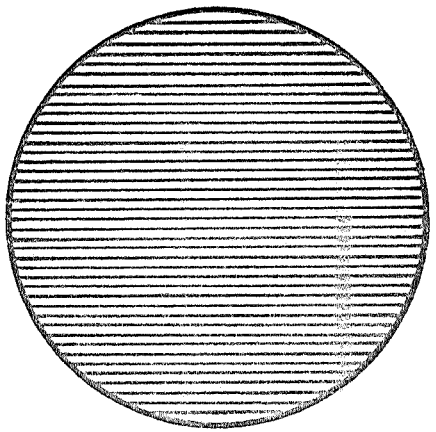

RONCHI RULING: Parallel lines scribed and inked on an optically flat glass disk such that 50% of the area is opaque and 50% is transparent.

FIGURE 6 - Ronchi Ruling

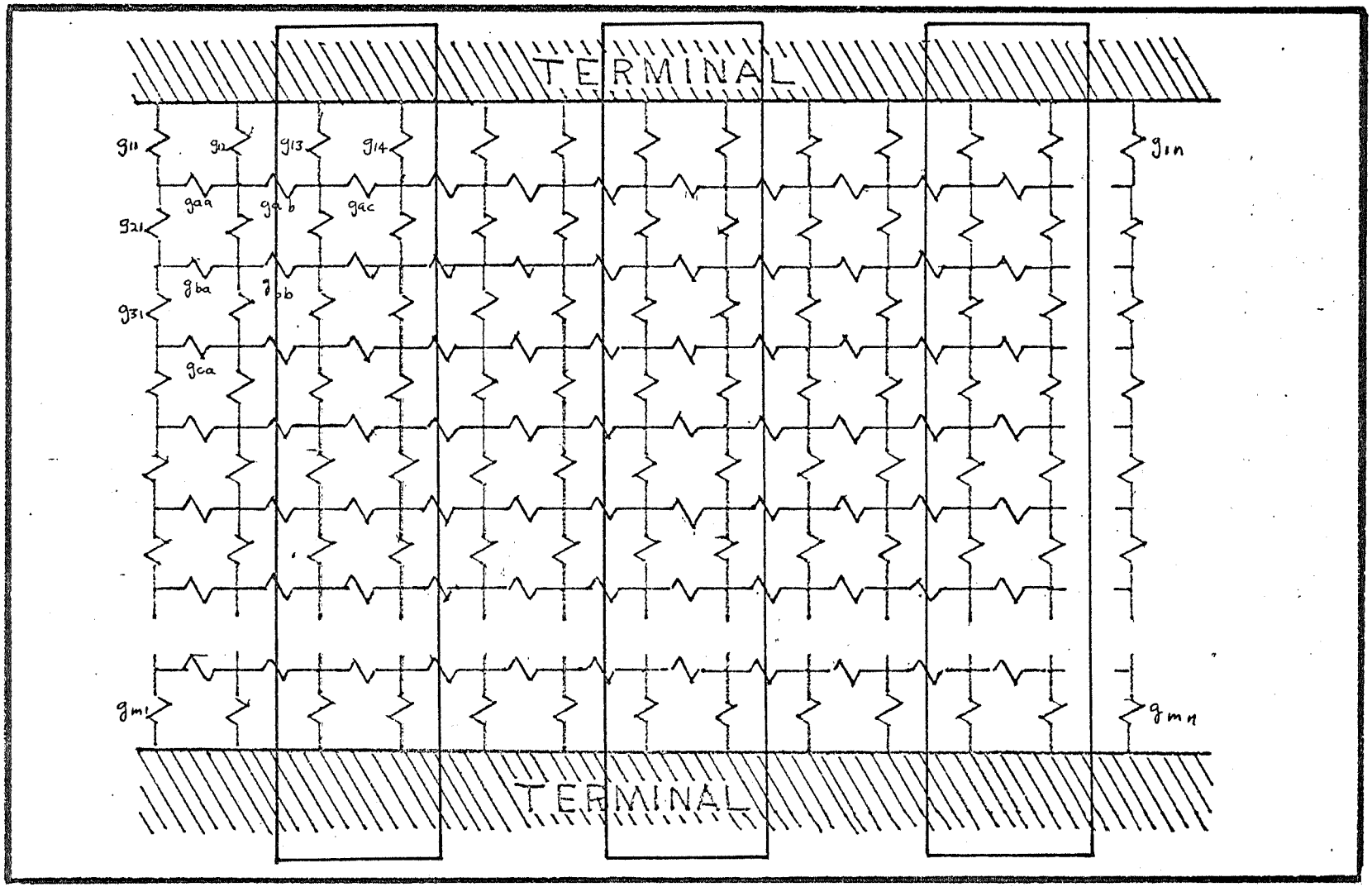

FIGURE 7 - Matrix with Perpendicular Line Image

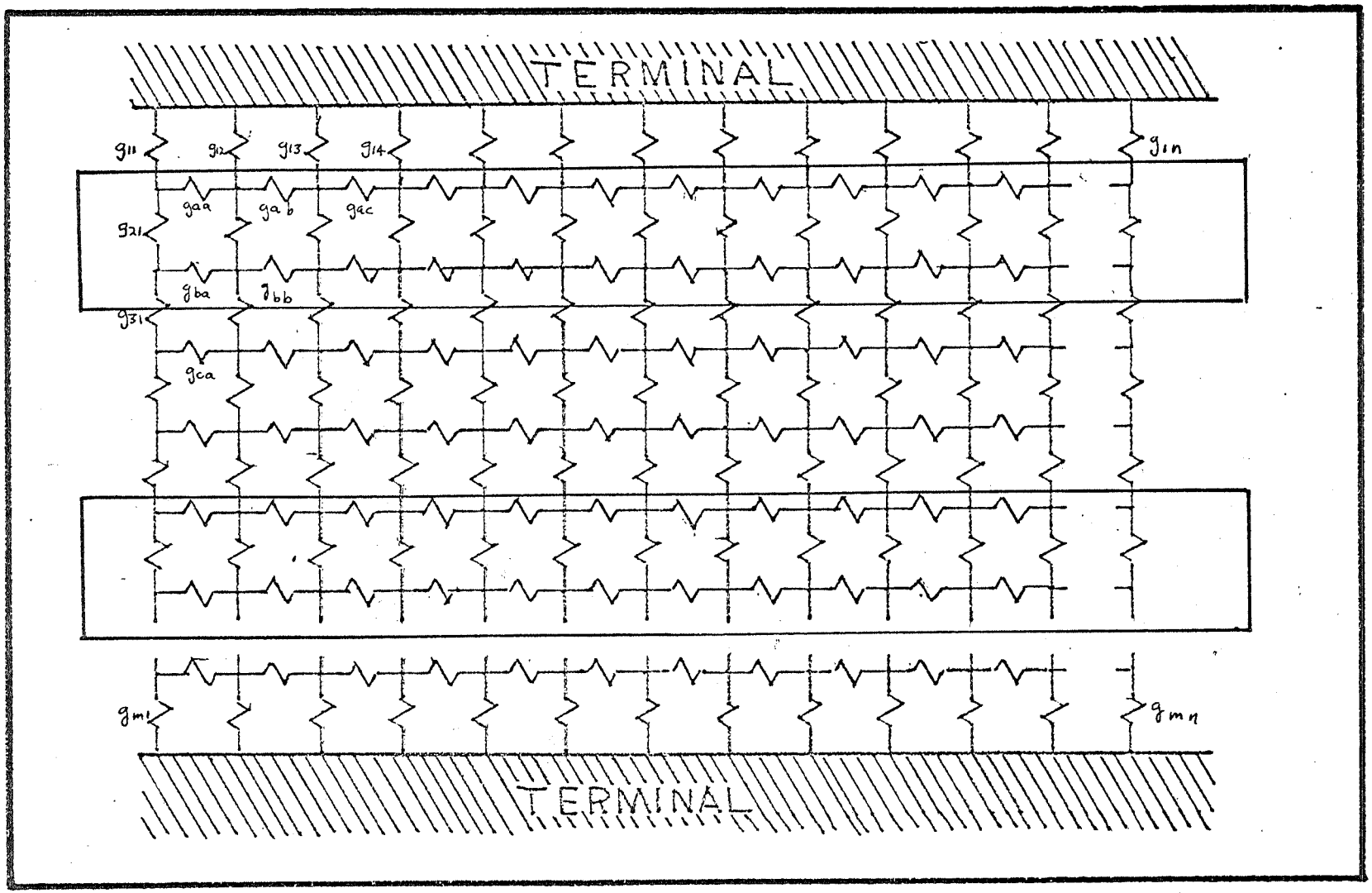

FIGURE 8 - Matrix with Parallel Line Image

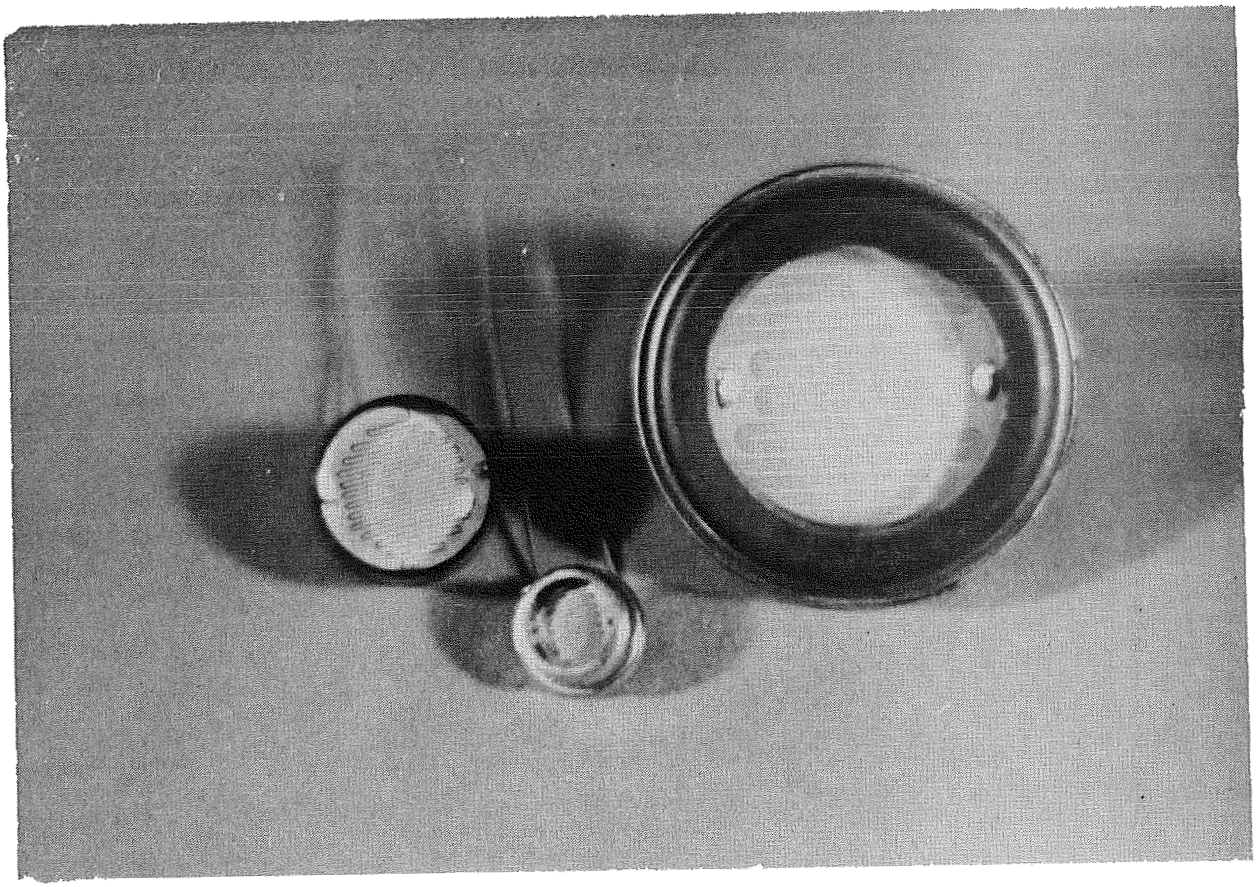

Figure #9 "Serpentine" Cells

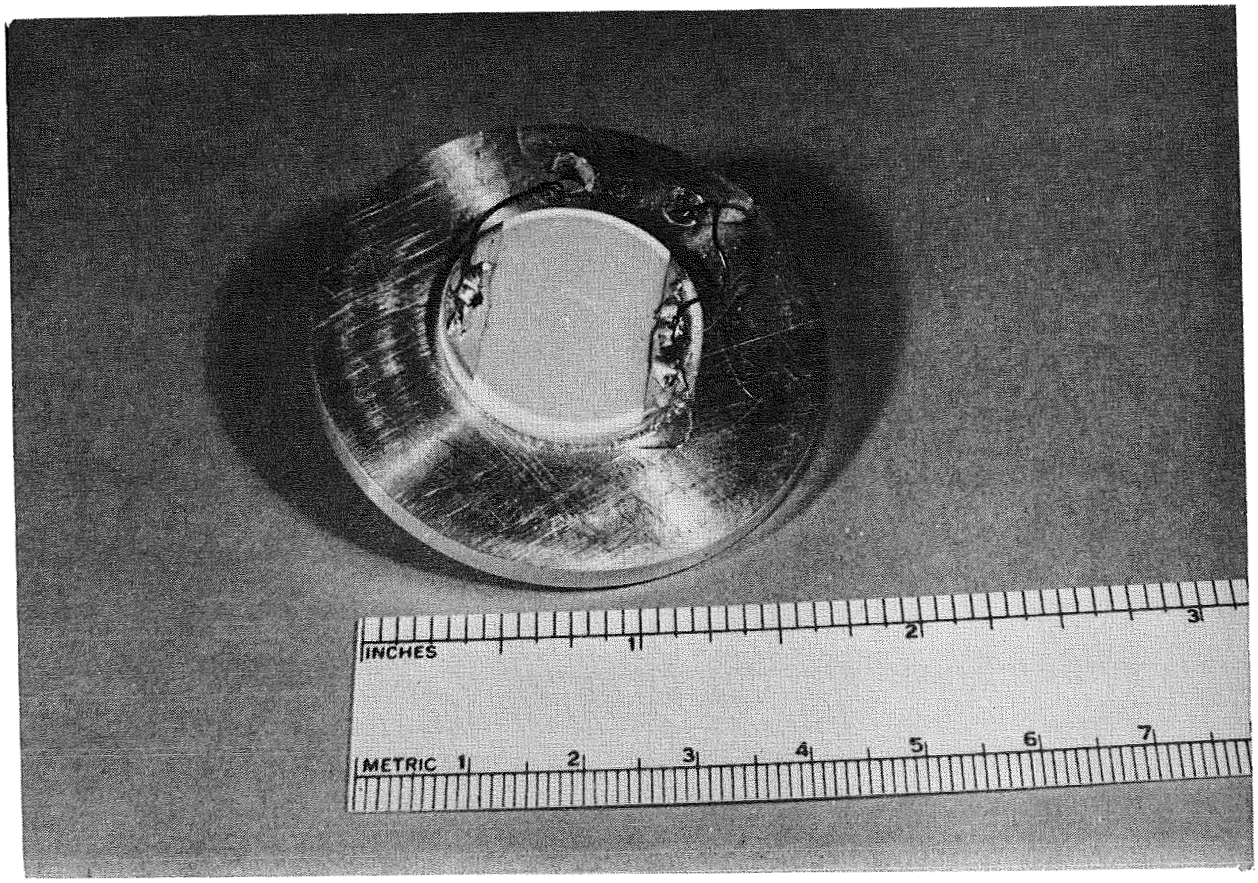

Figure #11 "Area" Cell

Figure #10 Experimental Setup

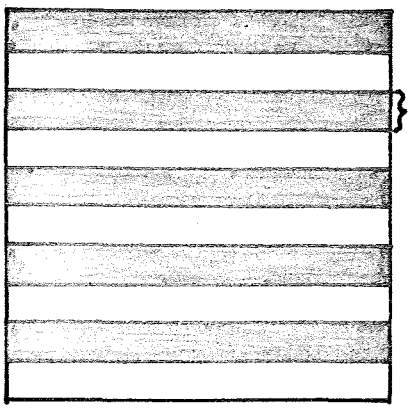

(a) Typical Straight Line Target

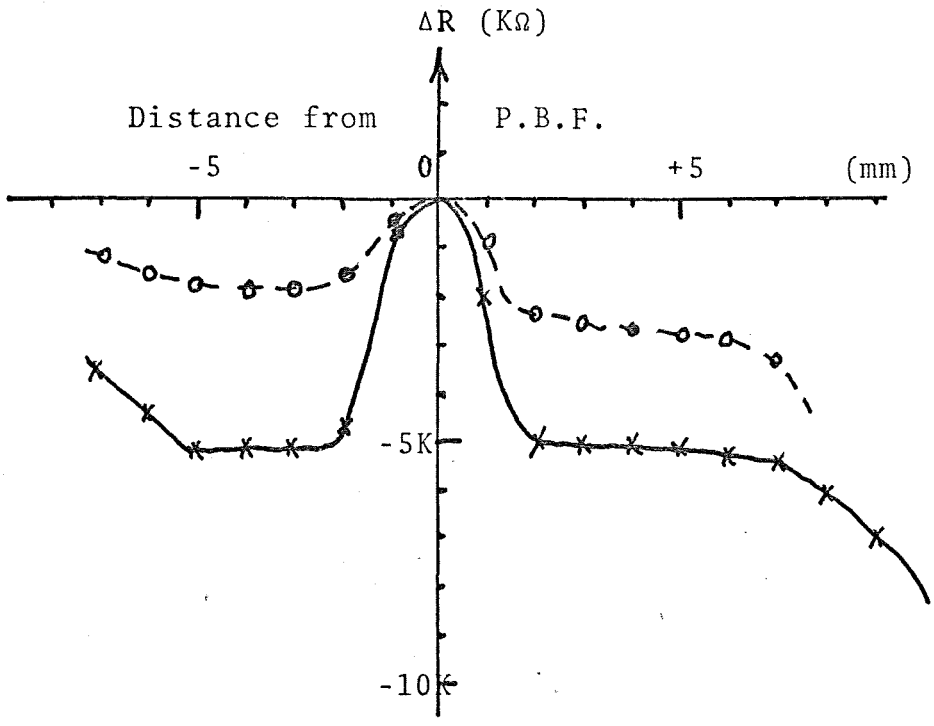

(b) Variation of Terminal Resistance as Cell is Moved through P.B.F.

FIGURE 12 - Response of "Serpentine" Cell to a Straight Line Target

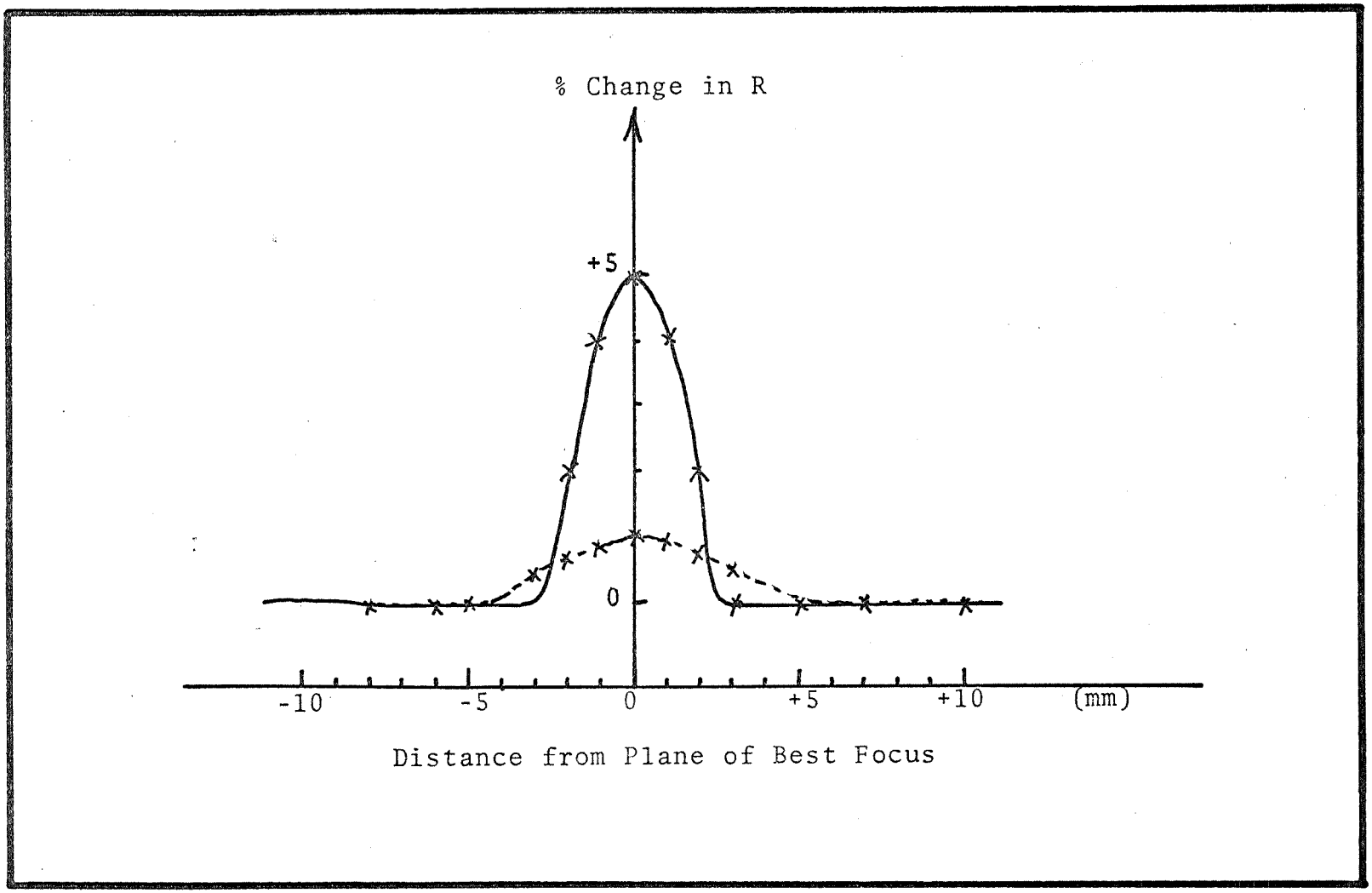

FIGURE 13 - Response of "Area" Cell to a Line Target

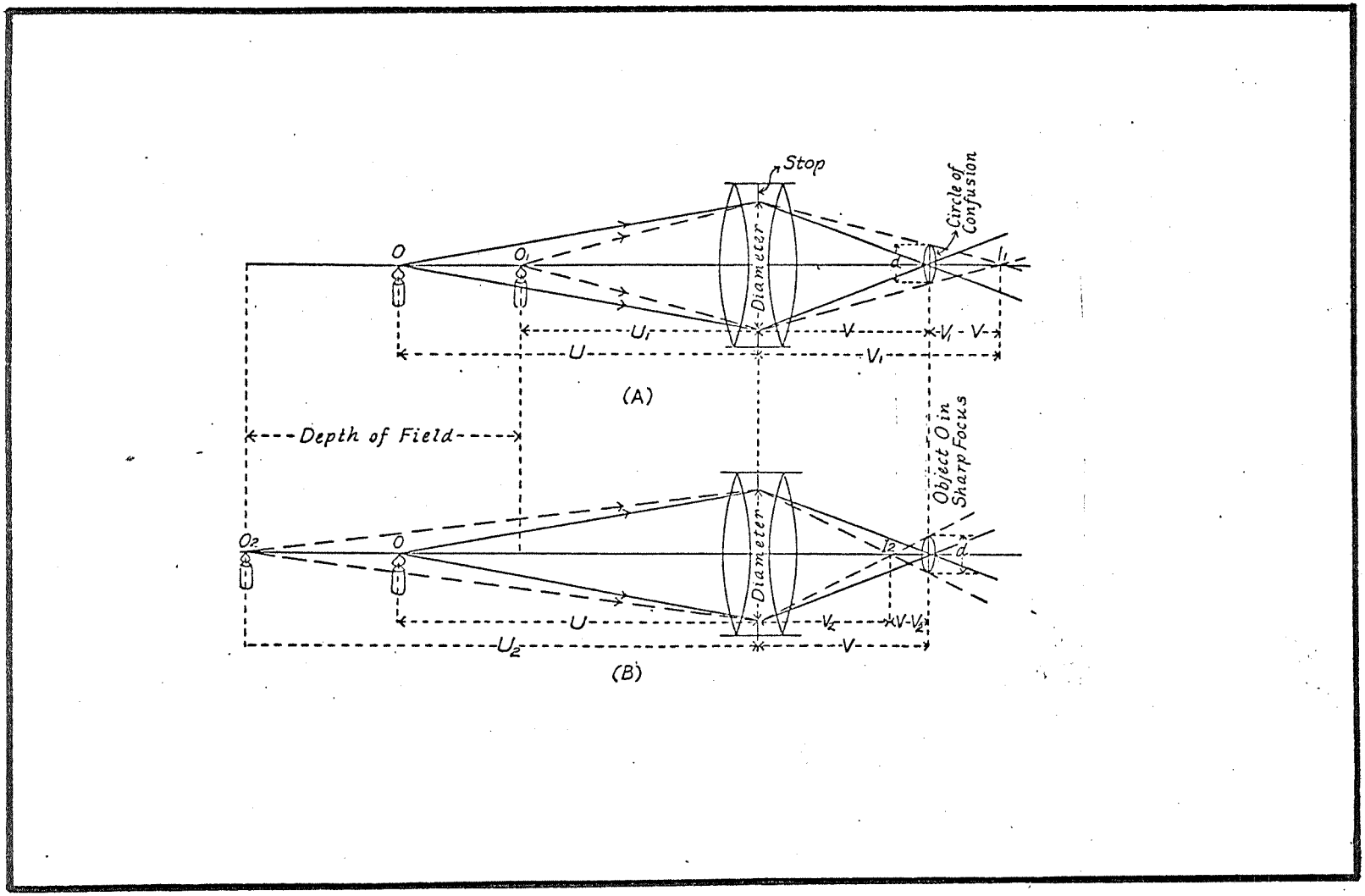

FIGURE 14 - Depth-of-Field Relations in a Single Lens

APPENDIX I - DERIVATION OF OPTICAL RELATIONSHIPS

(a) Derivation of Eqn. (3)

From Fig. 14 it is apparent that

$$\frac{D}{V_2} = \frac{d}{V - V_2} \tag{A1}$$

Using Eqn. (1) with U_2 and V_2 gives

$$V_2 = \frac{U_2 F}{U_2 - F} \tag{A2}$$

which, when substituted into Eqn. (A1), yields

$$D = d \frac{U_2 (U - F)}{F (U_2 - U)} \tag{A3}$$

(b) Proof that the far depth-of-field $(U_2 - U)$ exceeds the near depth-of-field $(U-U_1)$.

An expression similar to Eqn. (A3) involving U_1 rather than U_2 can be obtained by starting with

$$\frac{D}{V_1} = \frac{d}{V_1 - V} \tag{A4}$$

and using Eqn. (1) with U_1 and V_1 to get

$$D = d \frac{U_1 (U - F)}{F (U - U_1)} \tag{A5}$$

If the right-hand sides of Eqns. (A3) and (A5) are equated, it follows that

$$\frac{U_1}{U_2} = \frac{U - U_1}{U_2 - U} \tag{A6}$$

Because $U_1 < U_2$, one has that

$$(U - U_1) < (U_2 - U) \tag{A7}$$

which is the desired result.

APPENDIX II - PHOTOCELL SOURCES

(a) Small 1/4 x 1/4 inch "area cell":

Photomechanics Inc., 15 Stepar Pl.

Hungtinton Sta., L.I., New York 17746

(b) Large 1 inch diameter "area cell":

Ratio Corporation of America

Components Division, Harrison, N.J.

This cell is similar to the RCA 4404 cell before metalization.

APPENDIX III - DERIVATION OF CONDUCTANCES

Throughout the discussion it is assumed that the elements parallel to the terminals of the conductor matrix have negligible effects upon the conductance between terminals.

Case (i)

The conductance (G_s) of a vertical strip of n elements perpendicular to the terminal is:

$$G_s = \frac{g_o L}{n}$$

where q_o is the conductivity of each elemental conductor in darkness, and L is the illuminance.

The total conductivity (G_T) of m strips is:

$$G_T = G_s \, m$$

which yields Eqn. (8).

Case (ii)

If L_D is the illuminance of the dark lines of the image, the conductance due to m/2 vertical strips of n elements each, illuminated in this manner is:

$$G_D = g_o \, L_D \, \frac{m}{2n}.$$

In like manner, if L_L is the illuminance of the light lines of the image, the conductance due to this illumination is:

$$G_L = g_o \, L_L \, \frac{m}{2n}.$$

Total conductance due to both types of lines in the image

is merely the sum of the two,

$$G_T = g_o\left(\frac{m}{n}\right)\frac{1}{2}\,(L_D + L_L).$$

Case (iii) (ruling lines parallel to terminal electrodes).

Again if L_D and L_L are the respective illuminences of the lines in the image, the resistance of a vertical strip of n elements, half of which are illuminated by L_D and half of which are illuminated by L_L is:

$$R_s = \frac{n}{2}\,\frac{r_o}{L_D} + \frac{n}{2}\,\frac{r_o}{L_L}$$

where $r_o = \frac{1}{g_o}$.

The conductance of this strip is:

$$G_s = \frac{1}{\frac{n\,r_o}{2}\left(\frac{1}{L_D} + \frac{1}{L_L}\right)}.$$

and the conductance of m such strips is:

$$G_T = \frac{2m}{nr_o}\left[\frac{1}{\frac{1}{L_D} + \frac{1}{L_L}}\right]$$

$$= 2\left(\frac{m}{n}\right)g_o\left[\frac{L_o\;L_L}{L_D + L_L}\right].$$

REFERENCES

1. Wright, Jack K., Jr., "Mars Rover Close-Range Obstacle Detection", NASA NGL 33-018-091, May 1968.

2. Burns, Richard H., Bendor, Jonathon, Trested, Warren C., Jr., "Electromagnetic Obstacle Sensors", NASA NGR 33-010-055, June 1968.

3. Boucher, Paul E., Photography, New York, Van Nostrand. 1955, p. 34-60.

4. Pargas, Paul, "Phenomena of Image Sharpness Recognition of CdS and CdSe Photoconductors", Journal Opt. Soc. of Amer. 54, no. 4, p. 516-519, 1964.

5. Craig, Dwin R., "Image Sharpness Meter", Phot. Sci. Eng., 5, no. 6, p. 337-342, 1961.

6. Hadley, C.P., and Fisher, S.E., RCA Review, 20, p. 640, 1959.

7. Aulatta, John, Private Communication, Photomechanisms Inc.